J Optim Theory Appl (2017) 174:818–836
DOI 10.1007/s10957-017-1134-z

# A Comprehensive Differential Game Theoretic Solution to a Game of Two Cars

**Ritwik Bera**[1] · **Venkata Ramana Makkapati**[2] · **Mangal Kothari**[3]

Received: 27 August 2016 / Accepted: 27 June 2017 / Published online: 5 July 2017


**Abstract** In this paper, a pursuit-evasion game involving two non-holonomic agents is examined using the theory of differential games. It is assumed that the two players move on the Euclidean plane with fixed but different speeds and they each have a lower bound on their achievable turn radii. Both players steer at each instant by choosing their turn radii value and directions of turn. By formulating the game as a *game of kind*, we characterize the regions of initial conditions that lead to capture as well as the regions that lead to evasion, when both the players play optimally. The game is then formulated as a *game of degree* to obtain time-optimal paths for the pursuer and evader inside a capture region. Besides, all possible scenarios are considered for both players that differ in speed ratios and maneuverability constraints. Solutions are provided for those cases using appropriate simulation parameters, which aid in understanding the characteristics of the game of two cars under a wide range of constraints.

Communicated by Bruce A. Conway.

✉ Mangal Kothari
mangal@iitk.ac.in

Ritwik Bera
britwik@iitk.ac.in

Venkata Ramana Makkapati
mvramana@gatech.edu

1 Department of Mechanical Engineering, Indian Institute of Technology Kanpur, Kanpur 208016, India

2 School of Aerospace Engineering, Georgia Institute of Technology, Atlanta, GA 30332-0150, USA

3 Department of Aerospace Engineering, Indian Institute of Technology Kanpur, Kanpur 208016, India

**Keywords** Differential games · Min–Max strategies · Non-holonomic constraints · Barriers · Collision avoidance

## 1 Introduction

Two-player pursuit-evasion (PE) games have been studied since early 1950s for their civilian and strategic applications. They can be solved using a differential game formulation [1–3]. The associated Hamilton–Jacobi–Isaacs (HJI) partial differential equation has to be solved in this regard to obtain optimal strategies for both players. A multitude of formulations ranging from games between point robots [4] to games between spacecrafts [5], dogfight between missile and aircraft [6] have been widely studied [7]. Additionally, PE games have also been discussed under exogenous disturbances using flow fields by Sun and Tsiotras [8]. The unparalleled efficiency of the Isaacs' approach, in solving a two-player PE game, can be observed in the aforementioned works. Though this method is known for its accurate results, it suffers from the *curse of dimensionality*. Hence, it cannot be used for games involving three or more pursuers as it can become computationally intensive.

One of the most widely studied PE games is the *Homicidal Chauffeur* game, involving a completely agile evader and a non-holonomic pursuer [1]. A scenario where both the players have non-holonomic kinematics is a natural extension to the Homicidal Chauffer game, that is studied under the title *A Game of Two Cars*. This extension has been previously explored but with different approaches. The game drew attention due to its practical significance and also because of the underlying fact that all realistic vehicles have non-holonomic constraints. Moreover, in today's age of information technology, the dynamics of a vehicle can be modeled to higher degree of precision and the optimal control inputs can be chosen accordingly.

The game of two cars was introduced by Isaacs, formulated as game of kind, and a solution was provided for one of the many cases possible. The considered case dealt with the speeds of the players [1]. Later, a game between two aircraft was studied and solutions were obtained using a trajectory template method [9]. Subsequently, a stochastic version of the game was analyzed by Yavin and De Villiers [10]. A strategy based on proportional navigation (PN) guidance was conceived in this regard, and piecewise programming strategy was used as a solution technique [11]. A version with multiple non-holonomic pursuers was solved using the idea of safe-reachable areas and Dubins distance [12]. The game considered players with identical dynamics and presented approximate solutions by utilizing certain classical missile guidance laws [13]. Recently, the game was analyzed for the case of high speed evaders [14,15].

There are also approaches, based purely on geometry, that have been used to solve the game of two cars [16,17]. Using a geometric approach, the game was extended to a three-dimensional setting by Rublein [18]. A variant of the game where both the players had identical speeds and turn radius constraints was studied by Getz [19]. Eventually, Pachter and Getz solved the two target version of the game [20]. However, these geometrical approaches compromised on optimality.

Although the game of two cars has received attention in the past, there does not exist an all-encompassing and comprehensive analysis of the game that covers all possible

scenarios relating to the speed and maneuverability of both players. In the current literature on the game of cars, the analyses on various cases are shared between game theoretic and geometric approaches. While the geometry-based approaches compromise on optimality, the game theoretic approach provides accurate results. In this paper, a single theoretical framework is adopted to analyze all the possible cases pertaining to the speed and maneuverability constraints. The analyses, presented in this paper, can be seen as a broad extension to the work done by Pachter et al. on barrier surfaces [17,21]. It includes 3D visualizations of the state space, demonstrating various classes of barrier and switching surfaces, for all possible scenarios. The results and inferences obtained in this paper can be applied to the work done in Ref. [22] to create a realistic collision avoidance game where an aircraft wish to avoid a collision with another aircraft.

The rest of the paper is organized as follows. Section 2 formally describes the problem formulation dealt in this paper. Section 3 develops a mathematical theory for the game. It presents analytical solutions of the equations concerning the game of kind and the game of degree. Section 4 presents solutions of the game under various constraints. Simulation results are discussed under certain test conditions that provide useful interpretations for different cases. Section 5 presents concluding remarks and the scope for future work.

## 2 Problem Formulation

Consider a pursuer and an evader moving on the Euclidean plane. The subscripts $p$ and $e$ are used for the pursuer and the evader, respectively. The pursuer's objective is *capture*: to reach a state where it is within the radius of capture of the evader ($\ell$), whereas the evader's target is *evasion*: a state in which it avoids capture indefinitely.

The dynamics of the players, written in an inertial frame of reference, are given by

$$\begin{aligned} \dot{x}_p &= v_p \cos\theta_p,\ \dot{y}_p = v_p \sin\theta_p,\ \dot{\theta}_p = -\frac{v_p}{R_p}\psi, \\ \dot{x}_e &= v_e \cos\theta_e,\ \dot{y}_e = v_e \sin\theta_e,\ \dot{\theta}_e = -\frac{v_e}{R_e}\phi, \end{aligned} \tag{1}$$

where $(x_p, y_p),\ (x_e, y_e) \in \mathbb{R}^2$ are the positions of the players, and $\theta_p,\ \theta_e \in [0, 2\pi)$ are the corresponding heading angles. $v_e,\ v_p$ denote the speeds, and $R_p,\ R_e$ denote the minimum turn radii of the players. $\psi,\ \phi \in [-1,\ 1]$ are the control inputs of the pursuer and the evader, respectively. It can be seen that for a given set of initial conditions at time $t = 0$, the game evolves in the six-dimensional state space. However, it can be analyzed in a three-dimensional (3D) *reduced state space*, as described below.

### 2.1 Differential Game Formulation in the Reduced State Space

The problem is transformed from the six-dimensional game space to the three-dimensional reduced state space at first by fixing the origin of a rotating coordinate

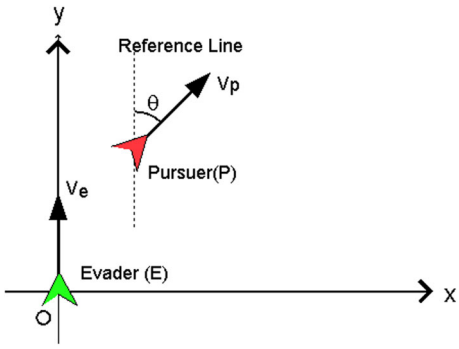


**Fig. 1** Players in the reduced state space

frame at evader's current position, and then by aligning its $y$-axis with evader's velocity vector, see Fig. 1. The dynamics, with the state vector $\mathbf{x} = [x\ y\ \theta]^\top$, can then be expressed as

$$\begin{aligned} \dot{x} &= v_p \sin\theta - \frac{v_e y \phi}{R_e}, \\ \dot{y} &= v_p \cos\theta - v_e + \frac{v_e x \phi}{R_e}, \\ \dot{\theta} &= -\frac{v_e \phi}{R_e} + \frac{v_p \psi}{R_p}, \end{aligned} \tag{2}$$

where $(x, y) \in \mathbb{R}^2$ refers to the position of the pursuer relative to the evader in the rotating frame, $\theta \in [0, 2\pi)$ is the pursuer's relative heading in the new reference frame, given by $\theta = \theta_e - \theta_p$. The game evolves in the reduced state space, given the initial condition $\mathbf{x}(0) = \mathbf{x}_0 \in \mathbb{R}^2 \times [0, 2\pi)$, and it terminates when the pursuer enters a cylindrical region of capture, $\mathcal{B} \in \mathbb{R}^2 \times [0, 2\pi)$, of radius $\ell$ and length $2\pi$. The *terminal surface* $\mathcal{C}$ is the manifold in the state space which once penetrated, determines the termination of a game. The terminal surface is thus the surface of the cylinder in the reduced state space, whose radius is $\ell$ and its axis is along the $\theta$-axis.

The motivation behind keeping the reference frame's origin fixed at the evader is that the solutions will help in knowing the initial states of the pursuer (relative to the evader) which can lead to successful evasion. Such a representation is useful in collision avoidance applications.

Now, the payoff function is defined as

$$J_k(\mathbf{x}_0, \psi, \phi) = \begin{cases} +1 & \text{for escape,} \\ 0 & \text{for neutral outcome,} \\ -1 & \text{for capture.} \end{cases} \tag{3}$$

The subscript $k$ is used to denote that the formulation is a game of kind. For a given initial condition, the pursuer tries to minimize the payoff, whereas the evader strives to maximize the payoff, using their respective control inputs. If the pursuer's path in the reduced state space intersects $\mathcal{C}$ but does not penetrate it, then the outcome is neutral. Our primary goal is to find zones in the 3D game space that enclose initial

states leading to either capture or evasion. Accordingly, to classify the initial states, the game is originally formulated as a game of kind.

## 3 Problem Analysis

### 3.1 Game of Kind

The game is solved by utilizing the theory put forth by Isaacs [1]. The first step is to find the *usable part* of the terminal surface. The usable part is the portion of the terminal surface which when reached by a pursuer will lead to capture in the next time step under optimal play. All retrograde optimal paths that involve capture emanate from the usable part. The complement of the usable part on the terminal surface is the *non-usable part*. Under optimal play, the pursuer cannot immediately enforce capture on reaching any state in this part. The *boundary of usable part* (BUP) separates the usable part and the non-usable part on the terminal surface.

The surfaces separating the two zones are known as *barriers*, which are the loci of all the initial game states that lead to neutral outcome. Under optimal play, no set of control inputs can allow the trajectories to cross the barrier surface. In other words, the paths (defining the progression of the game) in the reduced state space will always be contained on one side of the barrier surface. In particular, barrier surfaces emanate from the BUP and are tangential to the terminal surface. By definition, the vector $[\dot{x}\ \dot{y}]^T$ at the usable part, under optimal play, should be pointing into the cylindrical capture region $\mathcal{B}$, i.e.,

$$\min_{\psi}\ \max_{\phi}\ x\dot{x} + y\dot{y} < 0, \tag{4}$$

which is the dot product between the vectors $[\dot{x}\ \dot{y}]^\top$ and $[x\ y]^\top$. Consequently, the BUP is obtained from the solution of the equation given below.

$$\min_{\psi}\ \max_{\phi}\ x\dot{x} + y\dot{y} = 0,\ (x, y) \in \mathcal{C}. \tag{5}$$

Moreover, the terminal surface $\mathcal{C}$ can be parameterized using the variables $s_1$ and $s_2$, where $(x, y, \theta) = (\ell \sin s_1, \ell \cos s_1, s_2)$. Now, using the dynamics presented in (2), the BUP can be expressed as

$$\sin s_1 (v_p \sin s_2) - \cos s_1 (v_e - v_p \cos s_2) = 0. \tag{6}$$

It can also be written as a dot product between $[(\sin s_1)\ (-\cos s_1)]^\top$ and $[(v_p \sin s_2)\ (v_e - v_p \cos s_2)]^\top$. Equation (6) provides two possible solutions of $s_1$, for a given $s_2$:

$$\sin s_1 = \pm\frac{v_e - v_p \cos s_2}{v}, \quad \cos s_1 = \pm\frac{v_p \sin s_2}{v}, \tag{7}$$

where $v = \sqrt{v_p^2 + v_e^2 - 2 v_e v_p \cos s_2}$.

Remarks: 1) It can be observed that the BUP always consists of diametrically opposite points on the terminal surface $\mathcal{C}$, regardless of the speeds of both players.
2) The position of a point along the BUP is also independent of the turn radius constraints of both players and also their control strategies. This is a consequence of both players having non-holonomic dynamics.

The *retrograde path equations* (RPEs) for the barrier surface can be now derived using the HJI equation, which is presented as the *Main Equation* in the book by Isaacs [1]. Defining a normal vector $[\nu_1\ \nu_2\ \nu_3]^\top \in \mathbb{R}^3$ at each point on the barrier surface that extends into the escape zone, the HJI equation for the game of kind can be expressed as

$$\min_{\psi}\ \max_{\phi}\ \sum_{i=1}^{3} \nu_i f_i = 0. \tag{8}$$

where $f_1$, $f_2$, and $f_3$ stand for the dynamics of $x$, $y$, and $\theta$, respectively, that are given in (2). Moreover, (8) can be fully expanded into the form,

$$\min_{\psi}\ \max_{\phi}\ v_p(\nu_1 \sin\theta + \nu_2 \cos\theta) + \frac{v_e}{R_e}(-y\nu_1 + x\nu_2 - \nu_3)\phi + \frac{v_p}{R_p}\nu_3\psi - v_e\nu_2 = 0, \tag{9}$$

and the optimal control strategies are identified as

$$\phi^* = -\operatorname{sgn}(A), \quad \psi^* = -\operatorname{sgn}(\nu_3), \tag{10}$$

where $A = y\nu_1 - x\nu_2 + \nu_3$, sgn(.) is the signum function. This is a classic example of *bang–bang control* where the control policy of a player switches between the extremes. At this point, constructing the barrier surface requires the information of how the normal vector $[\nu_1\ \nu_2\ \nu_3]^\top$ evolves in time, which is obtained using the equation

$$\dot{\nu}_k = -\min_{\psi}\ \max_{\phi}\ \sum_{i=1}^{3} \nu_i \frac{\partial f_i}{\partial x_k},\ k = 1, 2, 3, \tag{11}$$

and in this case, $[x_1\ x_2\ x_3] = [x\ y\ \theta]$ [1]. Combining (11), and the dynamics in (2) with optimal control inputs, the RPEs are constructed in the retrograde time direction. The retrograde time variable can be expressed as $\tau = t_c - t$, $t_c$ is the time-to-capture. RPEs are differential equations with respect to retrograde time $\tau$ and indicate the fact that the game is solved backwards in time from the terminal surface $\mathcal{C}$. Denoting the retrograde time derivative of a variable with "$\circ$" on its top, the retrograde evolution of the normal vector can be expressed as

$$\begin{aligned}
\overset{\circ}{\nu}_1 &= \frac{v_e\nu_2\phi^*}{R_e}, & \nu_1(\tau = 0) &= \sin s_1,\\
\overset{\circ}{\nu}_2 &= -\frac{v_e\nu_1\phi^*}{R_e}, & \nu_2(\tau = 0) &= \cos s_1,\\
\overset{\circ}{\nu}_3 &= v_p(\nu_1\cos\theta - \nu_2\sin\theta), & \nu_3(\tau = 0) &= 0.
\end{aligned} \tag{12}$$

Similarly, the retrograde evolution of the states can be expressed with a minus sign in front of their corresponding dynamics as

$$\begin{aligned}
\overset{\circ}{x} &= -\left(v_p \sin\theta - \frac{v_e y \phi^*}{R_e}\right), && x(\tau = 0) = \ell \sin s_1,\\
\overset{\circ}{y} &= -\left(v_p \cos\theta - v_e + \frac{v_e x \phi^*}{R_e}\right), && y(\tau = 0) = \ell \cos s_1,\\
\overset{\circ}{\theta} &= \frac{v_e \phi^*}{R_e} - \frac{v_p \psi^*}{R_p}, && \theta(\tau = 0) = s_2.
\end{aligned} \tag{13}$$

The initial conditions on the state denote a point on the BUP, where $s_1$ satisfies (7), and the initial conditions on the normal vector are realized from (9). The RPEs are integrated in reverse time for various point on the BUP, and the barriers formed indicate a set of backward reachable states from the BUP. All the states inside the usable part can be reached through the trajectories contained between the barrier surfaces. From the initial conditions specified earlier, it can be observed that $A = \nu_3 = 0$. Therefore, the optimal controls take the form

$$\phi^* = -\operatorname{sgn}(\overset{\circ}{A}), \quad \psi^* = -\operatorname{sgn}(\overset{\circ}{\nu}_3). \tag{14}$$

Furthermore, they can be written as

$$\phi^* = \pm \operatorname{sgn}(v_e - v_p \cos s_2), \quad \psi^* = \pm \operatorname{sgn}(v_e \cos s_2 - v_p). \tag{15}$$

Note that the BUP consists of two sets of points running in parallel which are diametrically opposite along the cylindrical terminal surface. Hence, the barrier surface appears as a pair. The plus/minus sign in (15) signifies the fact that for a given $s_2$, the optimal controls of each player on the two sets of barrier surfaces are opposite in sign.

### 3.2 Time-Optimal Paths in the Capture Region

Once it is determined that the game's initial state is in the capture region, a game of degree formulation can provide time-optimal paths for the players. In the case of a collision avoidance problem, this analysis will help in finding a maneuver for the evader that maximizes time-to-collision (capture time). The payoff function for this formulation is defined as

$$J_d(\mathbf{x}_0, \psi, \phi) = \int_0^{t_c} \mathrm{d}t. \tag{16}$$

Here, subscript $d$ for the payoff function represents that the formulation is a game of degree. Now, the HJI equation can be written under the presumption that there exists a value function $V(\mathbf{x})$ such that

$$\min_{\psi} \max_{\phi} \sum_{i=1}^{3} V_i f_i + G = 0, \tag{17}$$

where $G = 1$ denotes the incremental cost in the payoff function, and $V_i = \frac{\partial V}{\partial x_i}(\mathbf{x})$, $i = 1, 2, 3$. The row vector $[V_1\ V_2\ V_3]$ can be understood as the gradient of the value function. Furthermore, (17) can be expressed as

$$\min_{\psi} \max_{\phi}\ v_p(V_1 \sin\theta + V_2 \cos\theta) + \frac{v_e}{R_e}(-yV_1 + xV_2 - V_3)\phi + \frac{V_3 v_p \psi}{R_p} - v_e V_2 + 1 = 0. \tag{18}$$

Note that the optimal control inputs of the players remain unchanged, as given in (10). The dynamics of the gradient of the value function can be expressed as

$$\dot{V}_k = -\min_{\psi} \max_{\phi} \sum_{i=1}^{3} V_i \frac{\partial f_i}{\partial x_k} + \frac{\partial G}{\partial x_k},\ k = 1, 2, 3, \tag{19}$$

where $[x_1\ x_2\ x_3] = [x\ y\ \theta]$. Since $\frac{\partial G}{\partial x_k} = 0$, the RPEs are identical to those of game of kind, replacing $v_i$ with $V_i$, $\forall\, i \in \{1, 2, 3\}$. Note that the normal vector defined for the game of kind is analogous to the gradient of the value function. Since the expressions for the optimal control inputs remain the same, a similar logic, as employed in Sect. 3.1 , can be followed to specify the initial conditions. Given the initial conditions for the states as $\mathbf{x}(\tau = 0) = [\ell \sin s_1\ \ell \cos s_1\ s_2]^\top$, we specify

$$V_1(\tau = 0) = \delta \sin s_1,\ V_2(\tau = 0) = \delta \cos s_1,\ V_3(\tau = 0) = 0, \tag{20}$$

where $\delta$ is a parameter, obtained by plugging the initial conditions back into (18) and

$$\delta = \frac{-1}{v_p \cos(s_2 - s_1) - v_e \cos s_1}. \tag{21}$$

The original RPEs, (12) and (13), coupled with the new boundary conditions, (20) and (21), provide the time-optimal paths in the capture region.

## 4 Solutions and Interpretation

In this section, simulation results are presented for different cases based on the mathematical analysis carried out in the previous section. The radius of capture is set to $\ell = 0.5$, for all the cases that follow.

### 4.1 Case 1: Faster Evader ($v_p < v_e$)

For this case, the speeds of the players are considered to be $v_p = 0.6$, $v_e = 1$, and the minimum turn radii of the players are $R_p = R_e = 0.7$. Since, $v_e > v_p$,

$$\frac{v_e - v_p \cos s_2}{v} > 0\ \forall\, s_2,\ s_2 \in [0, 2\pi). \tag{22}$$

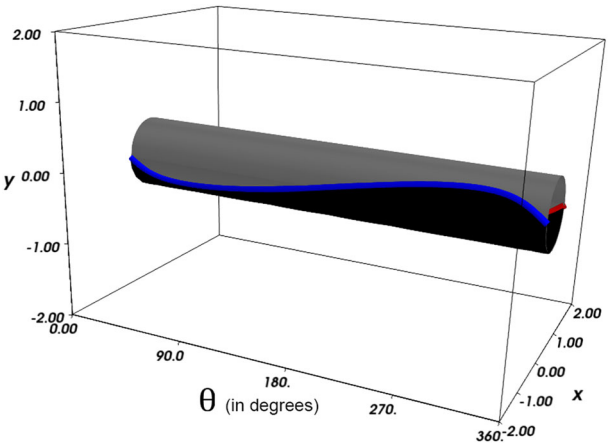


**Fig. 2** The usable part (*gray*) along with the BUP (*blue* and *red lines*) for a case of faster evader. The non-usable part is shown in *black*

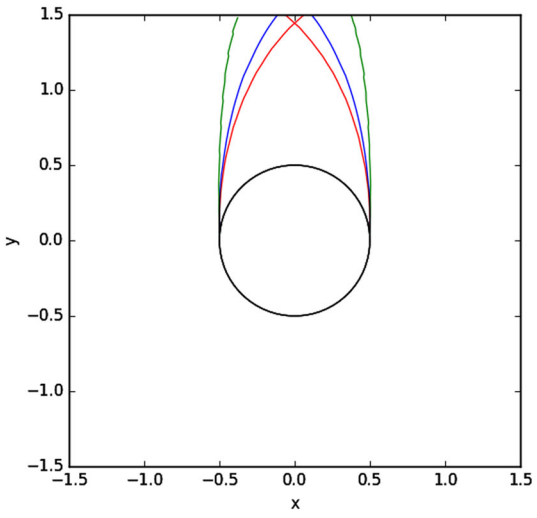


**Fig. 3** The effect of speed ratio on the capture zone for the case of a faster evader, shown by a cross section of the barrier surface cut at $\theta = 180°$. For the *red barriers*, $v_p = 0.6$, $v_e = 1.3$, for the *blue barriers*, $v_p = 0.6$, $v_e = 1$ and for the *green barriers*, $v_p = 0.6$, $v_e = 0.7$

Therefore, as shown in Fig. 2, the two curves representing the BUP stay on the either side of the plane x=0, throughout. The speeds, $v_e$ and $v_p$, govern the shape of those curves. As the speed ratio $\alpha = \frac{v_e}{v_p}$ increases, the BUP curves become more linear. At $\alpha \to \infty$, they happen to be straight lines, $s_1 = \pm\pi/2$, parallel to the $\theta$-axis on the terminal surface. This implies that when the evader is very fast compared to the pursuer, nominal changes in the pursuer's speed do not affect the outcome of the game, as the usable part and barrier stay roughly the same.

It is shown in Fig. 5 that the two sets of barrier surfaces intersect each other and create a bounded capture zone. Figure 3 shows that with an increase in the speed ratio $\alpha$, the volume of the capture zone in the 3D state space (and hence, the number of initial game states leading to capture) decreases. Figure 4 shows that as the minimum

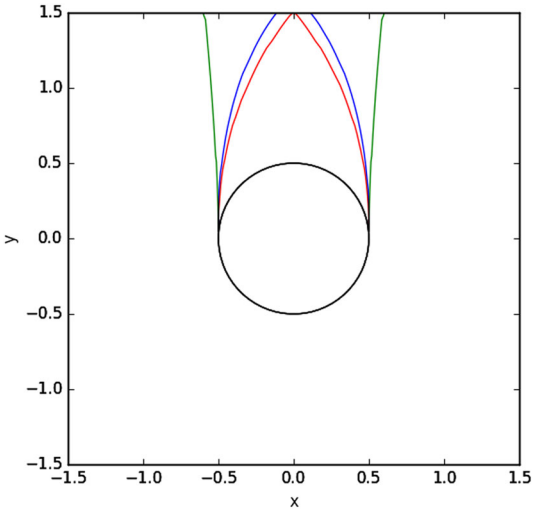


**Fig. 4** The effect of turn radius constraint ratio on the capture zone for the case a of faster evader, shown by a cross section of the barrier surface cut at $\theta = 180°$. For the *red barriers*, $R_p = 3$, $R_e = 0.7$, for the *blue barriers*, $R_p = 0.7$, $R_e = 0.7$ and for the *green barriers*, $R_p = 0.7$, $R_e = 3$

turn radius ratio $\beta = \frac{R_p}{R_e}$ increases, the two barrier surfaces converge while effectively reducing the volume of the capture zone. In the case of a highly agile pursuer and an evader with very low agility, the capture zone becomes unbounded. This phenomenon can be observed for the green barrier surfaces in Fig. 4. In a realistic sense, if the pursuer's and the evader's velocity vectors are towards each other, then the evader would not be able to turn fast enough to change its orientation away from the pursuer and will be captured.

It can be observed that $x = 0$ is the plane of symmetry, see in Figs. 3, 4, and hence, the barrier surfaces meet at the y-axis. This enables us to define a maximum time-to-capture $\tau_m$ that the evader can achieve in the capture zone. Let $f_x(\tau)$ denotes the x-coordinate of any of the retrograde optimal paths belonging to the barrier surfaces (that leads to neutral outcome). Then, the solution to the equation

$$f_x(\tau_m) = 0, \tag{23}$$

gives us the maximum time-to-capture $\tau_m$ in a single-pursuer problem.

Since $v_e > v_p$, and close to the terminal surface, on the barriers, $\psi^*$ is given by

$$\psi^* = \pm \operatorname{sgn}(v_e \cos\theta - v_p), \tag{24}$$

the optimal control strategy for the pursuer changes abruptly at $\theta = S$ and $\theta = 2\pi - S$ on both curves, where $S = \cos^{-1}\frac{v_p}{v_e}$. Also, the slope of $\overset{\circ}{\theta}$ is different at $\theta = S$, where it is positive, and at $\theta = 2\pi - S$, where it is negative. Particularly, in the case of the BUP lying on the left side of the plane $x = 0$, the two *classes* of optimal paths (orange and red in Fig. 5) close to $\theta = 2\pi - S$ (306.87°), emanating from either side, intersect and their retrogressive integration is curtailed beyond their intersection points. This leads to the formation of a *dispersal surface*.

At every point on the dispersal surface, the pursuer can choose between two optimal control inputs which will steer the game in such a way that time-to-capture remains the

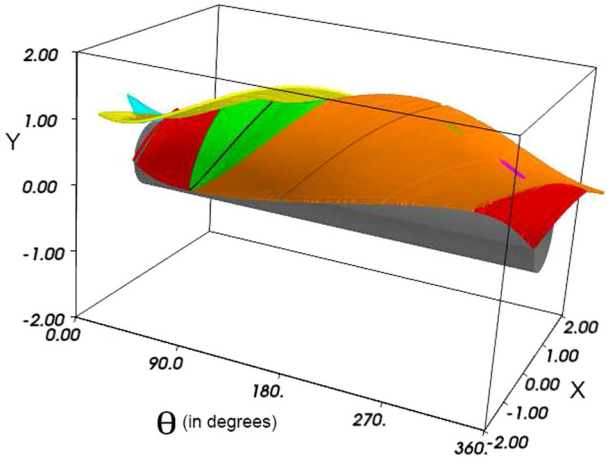


**Fig. 5** Figure depicting various classes of paths forming surfaces for a case of faster evader. The *black line* corresponds to universal surface. The surfaces shown in *orange* and *red* are combining to create a dispersal surface

same for both choices. Hence, this is a surface on which a player can employ mixed strategy. Let the x-coordinates of the any two retrograde optimal paths emanating from either sides of the dispersal surfaces be $f_x(.)$ and $g_x(.)$, functions of $\tau$. Similarly, the y-coordinates of the corresponding optimal paths be given by $f_y(.)$ and $g_y(.)$. Then, the locus of all the points defined by $(x_d, y_d)$ such that

$$x_d = f_x(\tau) = g_x(\tau), \quad y_d = f_y(\tau) = g_y(\tau) \tag{25}$$

forms the dispersal surface.

Another type of switching surface that can be observed is a *universal surface*. The two classes of optimal paths (orange and red in Fig. 5) emanating from either side, close to $\theta = S$ (53.13°), diverge away from each other, creating a void. This void is not devoid of optimal paths that lead to game termination, and it is filled by two sets of tributary paths emanating along the universal surface. The tributary paths can be obtained using the set of RPEs given in (13). As the tributary paths emerge from the universal surface, the initial conditions vary accordingly. The tributary paths are shown in green in Fig. 5. Note that the two sets of tributary paths seamlessly merge with both classes of optimal paths on each side. The equations and analysis corresponding to the universal surface are presented below.

### *4.1.1 Deriving the Universal Surface*

Since the evader's optimal control $\phi^*$ is constant throughout the BUP, and the pursuer's control $\psi^*$ input changes at the points of discontinuity of optimal paths, the kinematic equations can be considered to be linear in $\psi^*$. Hence, they can be expressed in the form, $\dot{x}_i = \alpha_i \psi + \beta_i,\ i = 1, 2, 3$, where $\alpha_i,\ \beta_i,\ i = 1, 2, 3$ are constants. These kinematic equations can be plugged into the HJI equation, which takes the form

$$\min_{\psi} \sum_{i=1}^{3} \alpha_i v_i \ \psi + \sum_{i=1}^{3} \beta_i v_i = 0, \tag{26}$$

with the optimal control input being

$$\psi^* = -\operatorname{sgn}\left(\sum_{i=1}^{3} \alpha_i v_i\right). \tag{27}$$

For one set of tributary paths, $\psi^* = 1$, and for the other set $\psi^* = -1$. Therefore, $\sum_i \alpha_i v_i = 0$, on the universal surface. It implies that $\sum_{i=1}^{3} \beta_i v_i = 0$. Following Isaacs' necessary condition [1] for a universal surface of the *linear vectogram type*, we obtain

$$\begin{vmatrix} \alpha_1 & \alpha_2 & \alpha_3 \\ \beta_1 & \beta_2 & \beta_3 \\ \gamma_1 & \gamma_2 & \gamma_3 \end{vmatrix} = 0, \tag{28}$$

where $\gamma_i = \sum_j^3 (\alpha_{ij}\beta_j - \beta_{ij}\alpha_j)$, which can be fully expanded into the form

$$\begin{vmatrix} 0 & -\frac{v_e \phi^* y}{R_e} + v_p \sin\theta & -v_p \cos\theta \frac{v_p}{R_p} \\ 0 & -v_e + v_p \cos\theta + \frac{v_e \phi^* x}{R_e} & v_p \sin\theta \frac{v_p}{R_p} \\ \frac{v_p}{R_p} & \frac{-v_e \phi^*}{R_e} & 0 \end{vmatrix} = 0. \tag{29}$$

Evaluating the determinant,

$$\frac{v_e \phi^*}{R_e}(-y \sin\theta + x \cos\theta) - v_e \cos\theta + v_p = 0, \tag{30}$$

and differentiating it with respect to $\tau$, the following equation is obtained.

$$\left[\frac{v_e \phi^*}{R_e}(y \cos\theta + x \sin\theta) - v_e \sin\theta\right] \frac{v_p \psi^*}{R_p} = 0. \tag{31}$$

This implies that on the universal surface $\psi^* = 0$, as otherwise, the term in the square brackets in (31) has to be zero, which will in turn imply that $\dot{x} = \dot{y} = 0$, a static state. This leads to the RPEs for the universal surface given below.

$$\begin{aligned} \mathring{x} &= \frac{v_e \phi^* y}{R_e} - v_p \sin\theta, \\ \mathring{y} &= \frac{-v_e \phi^* x}{R_e} + v_e - v_p \cos\theta, \\ \mathring{\theta} &= \frac{v_e \phi^*}{R_e}. \end{aligned} \tag{32}$$

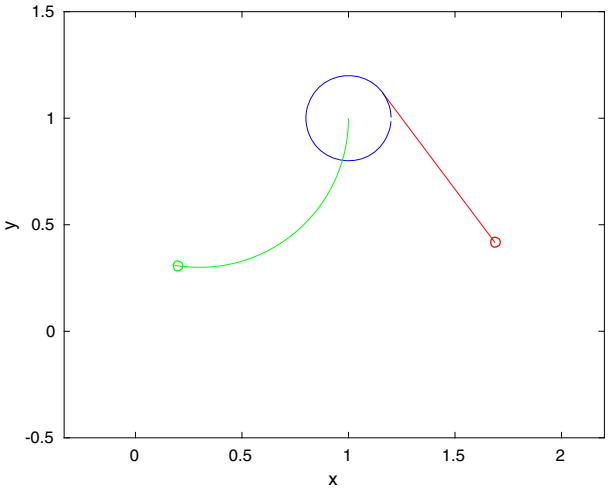


**Fig. 6** Trajectories of the players for a game progressing on a universal surface with radius of capture=0.2, $v_p = 0.6$, $v_e = 1$. The evader's trajectory is shown in *red*, and the pursuer's trajectory is shown in *green*

The physical implication is that on the universal surface, just before game termination, the pursuer is headed on a straight line path to intercept the evader while the evader is still performing a turning maneuver. This is shown in Fig. 6. It is interesting to note that the equations of $\overset{\circ}{x}$ and $\overset{\circ}{y}$, in (32), are exactly the same as the barrier equations for the *Suicidal Pedestrian Game* in Refs. [22] and [23].

### 4.2 Case 2: Equal Speeds ($v_p = v_e$)

In this subsection, a case where the players have equal speeds is analyzed. For this case, the speeds of the players are set to $v_p = 1$, $v_e = 1$, with their minimum turn radii being $R_p = R_e = 0.7$. The optimal control strategies for both the players are constant throughout the BUP, as can be observed from (15), given the fact that $v_e = v_p$. Thus, only a single class of surfaces exists along each of the curves that represent the BUP. Consequently, there are no switching surfaces in this case.

It is shown in Fig. 7 that the usable part (and hence the barrier surfaces) forms a spiral turn across the terminal surface $\mathcal{C}$. Note that the usable part is at different positions at 0 and $2\pi$. Figure 9 shows that the barrier surfaces fail to form completely enclosed capture zones in the reduced state space. Unlike the previous case, no universal surfaces are formed and the subsequent absence of tributary paths means that voids in the barrier surfaces along the $\theta$-axis remain unfilled. However, Fig. 8 shows that, similar to the previous case, as the minimum turn radius ratio $\beta$ increases, the size of the capture zone reduces and vice versa.

From Fig. 7, it can observed that at $\theta = 0$, the usable part suffers a discontinuity and abruptly shifts its location along $\mathcal{C}$. At $\theta = 0$, the value of $v$ in (7) is zero, and therefore, there is no usable part at $\theta = 0$. Physically, it can be interpreted as the fact that when both players have equal speed capabilities, there exists no capture which can

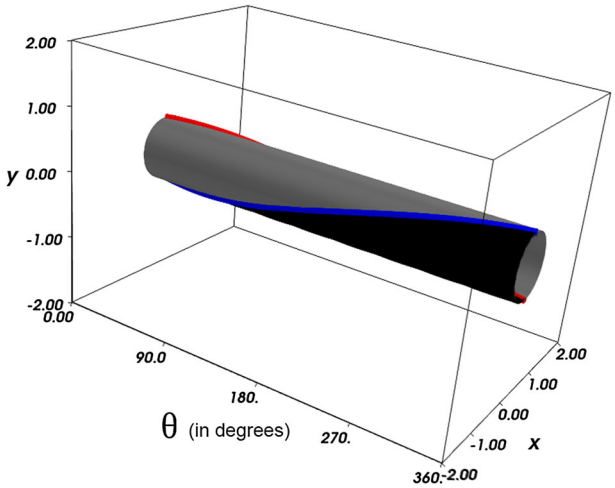


**Fig. 7** The usable part (*gray*) along with the BUP (*blue* and *red lines*) for a case of players with equal speeds. The non-usable part is shown in *black*

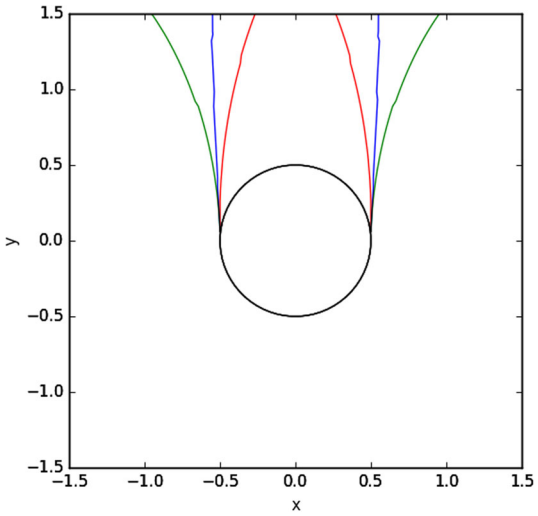


**Fig. 8** The effect of turn radius constraint ratio on the capture zone for the case of players with equal speeds, shown by a cross section of the barrier surface cut at $\theta = 180°$. For the *red barriers*, $R_p = 3$, $R_e = 0.7$, for the *blue barriers*, $R_p = 0.7$, $R_e = 0.7$ and for the *green barriers*, $R_p = 0.7$, $R_e = 3$

occur with their velocity vectors being parallel to each other. Hence, no state on the plane $\theta = 0$ can lead to capture. Consequently, the integration of the retrograde paths is curtailed at the $\theta = 0$ plane. Regardless of the superior agility of the pursuer, the capture zone in the state space is always bounded. This statement can be justified by the following example. Consider a case in the reduced state space where the game starts at an initial state with a sufficiently large value of y, i.e., the pursuer is far away. To ensure capture, the game must progress with an optimal path that leads from the initial state to the usable surface. However, as per the shape of the optimal paths (defined by the barrier surfaces), the path must cross $\theta = 0$ or $2\pi$. As explained earlier, this is not possible, since the integration of paths is curtailed at $\theta = 0$ plane. Consequently, even

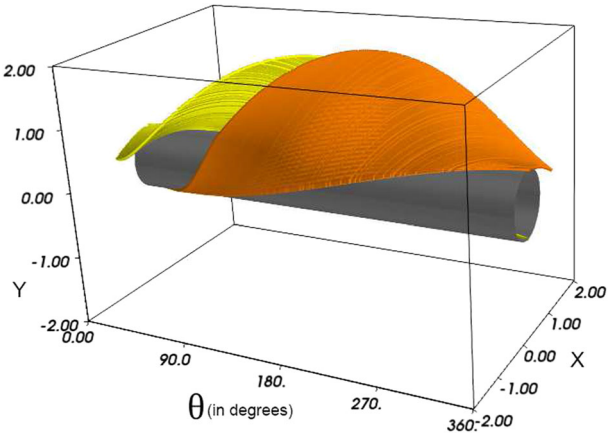


**Fig. 9** Figure depicting classes of paths forming surfaces for a case with players having equal speeds. The surfaces shown in *yellow* and *orange* are the two classes of surfaces in this case

if the barriers are diverging due to pursuer's maneuverability advantage, it is unable to provide an unbounded capture zone. This is physically manifested in the fact that if the pursuer is sufficiently far away from the evader, the evader has enough time to change its orientation and move away from the pursuer.

As shown in Fig. 9, due to the discontinuity in usable part, initial states with $\theta \to 0^-$ lead to capture in the first or the fourth quadrant, whereas initial states with $\theta \to 0^+$ lead to a capture state in the second or the third quadrants of the $x - y$ plane. In other words, only those initial states lead to capture wherein the pursuer's velocity vector is orientated almost in the direction of the evader's velocity vector, and the pursuer is sufficiently close to the evader. This is logical since if the pursuer is headed away from the evader, it will not be able to turn in the direction of the evader, that is equally fast, and capture it in finite time.

### 4.3 Case 3: Faster Pursuer ($v_p > v_e$)

For this case, the speeds of the players are considered to be $v_p = 1$, $v_e = 0.6$, and the minimum turn radii are $R_p = R_e = 0.7$. Since $v_p > v_e$, from (7), $s_1$ ranges from $-\pi/2$ to $\pi/2$. This can be observed in Fig. 10 as the BUP spirals around the terminal surface $\mathcal{C}$. The usable part traces back to the same positions at $\theta = 0$ and $\theta = 2\pi$, i.e., it is continuous at $\theta = 0$. Similar to the case of the faster evader, this case also showcases three different classes of optimal paths on each of the curves representing the BUP. This is because of the discontinuity in the optimal control strategy of the evader across the length of the BUP. The optimal control of the evader $\phi^*$ on the BUP is given by

$$\phi^* = \pm \operatorname{sgn}(v_e - v_p \cos\theta). \tag{33}$$

Since $v_p > v_e$, $\phi^*$ abruptly switches between +1 and -1 at $\theta = S$ and $\theta = 2\pi - S$, where $S$ in this case is $\cos^{-1}\frac{v_e}{v_p}$. The switching of $\phi^*$ leads to discontinuities in $\overset{\circ}{x}$, $\overset{\circ}{y}$

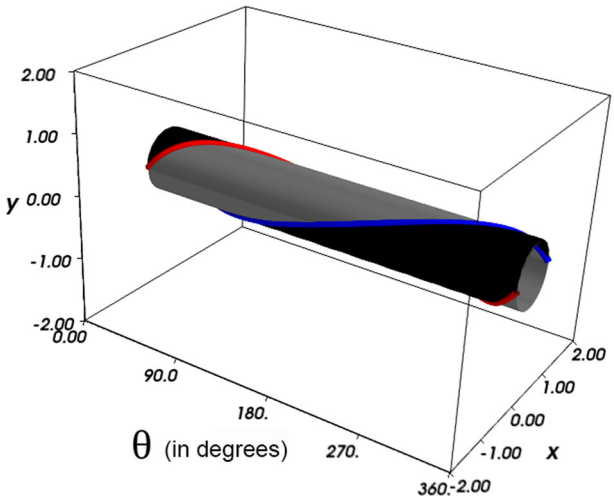


**Fig. 10** The usable part (*gray*) along with the BUP (*blue* and *red lines*) for a case of faster pursuer. The non-usable part is shown in *black*

and $\overset{\circ}{\theta}$, at the above-mentioned points. The dispersal surfaces in this case occur inside $\mathcal{B}$, which is why they are not considered relevant. On the other hand, universal surfaces extend outward from the terminal surface $\mathcal{C}$. Analogous to the case of the faster evader, the faster pursuer's optimal control $\psi^*$ remains constant across the BUP, whereas the slower evader's optimal control $\phi^*$ switches between +1/-1. Therefore, the kinematic equations on the universal surface are now linear in $\phi^*$. The discussion on the universal surface is presented below.

### *4.3.1 Derivation of the Universal Surface*

The derivation of universal surfaces in this case is identical to the one for the case of faster evader. The Isaacs' necessary analytic condition [1] provides the expression

$$\begin{vmatrix} \frac{-v_e y}{R_e} & v_p \sin\theta & \frac{v_e^2}{R_e} \\ \frac{v_e x}{R_e} & -v_e + v_p \cos\theta & 0 \\ -\frac{v_e}{R_e} & \frac{v_p \psi^*}{R_p} & 0 \end{vmatrix} = 0, \tag{34}$$

i.e.,

$$\frac{v_p \psi^* x}{R_p} + (-v_e + v_p \cos\theta) = 0. \tag{35}$$

After differentiating (35) with respect to $\tau$, the following equation is obtained that gives us the navigable RPEs.

$$\phi^* \left[ -\frac{v_e v_p \psi^* y}{R_p R_e} + \frac{v_e v_p}{R_p} \sin\theta \right] = 0. \tag{36}$$

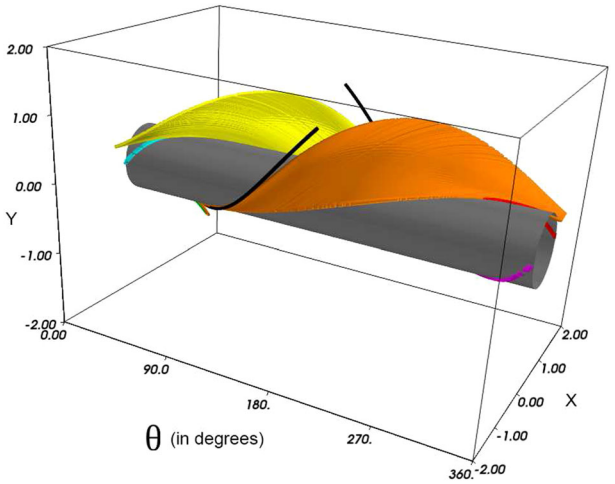


**Fig. 11** Figure depicting various classes of paths forming surfaces for a case of faster pursuer. The *black lines* corresponds to universal surfaces

If the expression in the square brackets in (36) is 0, it will imply that $\overset{\circ}{x} = 0$, $\overset{\circ}{y} = 0$, i.e., a static state. Thus, $\phi^* = 0$ on the universal surface.

Analogous to the case of faster evader, on the universal surface, just before the termination, the evader travels in a straight line, while the pursuer performs a turn to intercept it. Figure 11 shows that some of the barrier forming paths that originate from $\mathcal{C}$, where $0 < \theta < S$ (53.13°) and $2\pi - S$ (306.87°) $< \theta < 360°$, are contained in $\mathcal{B}$. Hence, they are discarded. Consequently, only one class of barrier-forming optimal paths exists along each curve representing the BUP. As the barrier surfaces fail to enclose a volume in the state space, the capture zone in this case is unbounded. In other words, the capture zone in this case is the entire state space because two classes of optimal paths (cyan and magenta) along the barrier are discarded. As a result of the non-existence of barriers emanating from certain portions of the BUP, there will exist spiraling paths leading from any state in the state space into the usable part. And, the barriers are no longer able to divide the state space into capture/escape zones.

It is important to note that for a very low $\beta$, magenta and blue-colored barrier-forming paths emanate outward from $\mathcal{B}$ and can no longer be discarded. Thus, there will exist some initial states which can lead to successful evasion, owing to the severe maneuverability disadvantage of the pursuer. As per Ref. [16], the entire state space will be a capture zone only if the following conditions are satisfied.

$$v_p > v_e, \quad \frac{v_p^2}{R_p} \geq \frac{v_e^2}{R_e}. \tag{37}$$

If the above condition is not satisfied, the surfaces formed by magenta and cyan colored classes of paths will lie completely outside $\mathcal{B}$ and emerge outwards into $\mathcal{E}$. These surfaces can then divide the state space into a capture and escape zone, see Fig. 12.

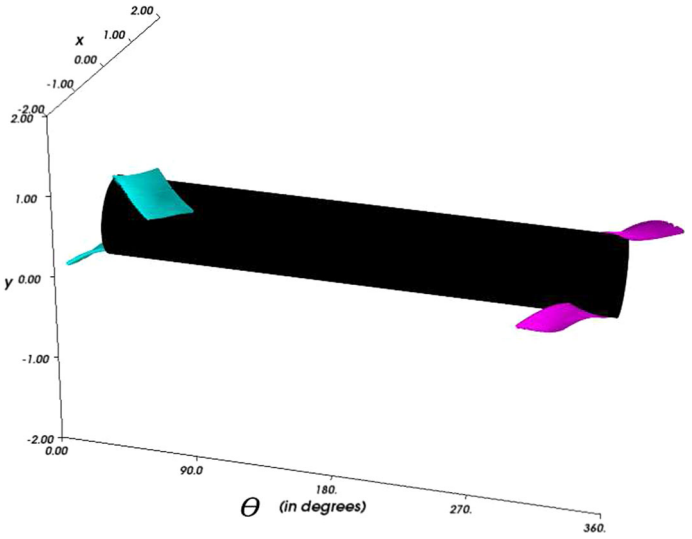


**Fig. 12** The new barrier surfaces that emanate from the manifold when Eq. 37 is not satisfied. Here $R_p = 3$, $R_e = 0.7$

Even when the barriers do not divide the state space into capture and escape zones, the barriers signify a discontinuity in the time to capture. This is because the barriers can not be crossed under optimal play. Hence, two pursuers starting at two different points that are equidistant to the evader may take different times-to-capture, if they are on either sides of the barrier.

## 5 Conclusions

The Game of Two Cars is studied in its entirety using Isaacs' theory of differential games. Using both game of kind and game of degree type formulations, time-optimal controls of both players are derived and the capture zones are analyzed. The nature of the barrier surfaces is examined under various assumptions on the speeds and the maneuverability constraints of the players. The equations corresponding to the switching surfaces, observed in the case of unequal speeds, are presented. The three-dimensional visualizations of the state space, showcasing the barrier and the switching surfaces for different scenarios, are demonstrated. The special features of the escape/capture zones are then compared. Follow-up work includes the study of the game under environmental disturbances, and a multi-pursuer version of the game.

## References

1. Isaacs, R.: Differential Games: A Mathematical Theory with Applications to Warfare and Pursuit, Control and Optimization. Wiley, New York (1965). Chapter 4,6,7,9
2. Ho, Y.C., Bryson, A.E., Baron, S.: Differential games and optimal pursuit-evasion strategies. IEEE Trans. Autom. Control **10**(4), 385–389 (1965). doi:10.1109/tac.1965.1098197

3. Evans, L.C., Souganidis, P.E.: Differential games and representation formulas for solutions of hamilton–jacobi–isaacs equations. Tech. rep, DTIC Document (1983)
4. Gu, D.: A differential game approach to formation control. IEEE Trans. Control Syst. Technol. **16**(1), 85–93 (2008)
5. Conway, B.A., Pontani, M.: Numerical solution of the three-dimensional orbital pursuit-evasion game. J. Guid. Control Dyn. **32**(2), 474–487 (2009). doi:10.2514/1.37962
6. Shinar, J., Gutman, S.: Three-dimensional optimal pursuit and evasion with bounded controls. IEEE Trans. Autom. Control **25**(3), 492–496 (1980). doi:10.1109/tac.1980.1102372
7. Grote, J.: The Theory and Application of Differential Games. D. Reidel. Publ, Dordrecht (1975)
8. Sun, W., Tsiotras, P.: Pursuit evasion game of two players under an external flow field. In: 2015 American Control Conference (ACC), pp. 5617–5622. Chicago, Illinois, USA (2015). doi:10.1109/acc.2015.7172219
9. Rajan, N., Prasad, U., Rao, N.: Pursuit-evasion of two aircraft in a horizontal plane. J. Guid. Control Dyn. **3**(3), 261–267 (1980). doi:10.1109/cdc.1975.270583
10. Yavin, Y., De Villiers, R.: Proportional navigation and the game of two cars. J. Optim. Theory Appl. **62**(3), 351–369 (1989)
11. Borowko, P., Rzymowski, W.: On the game of two cars. J. Optim. Theory Appl. **44**(3), 381–396 (1984). doi:10.1007/bf00935458
12. Kothari, M., Manathara, J.G., Postlethwaite, I.: A cooperative pursuit-evasion game for non-holonomic systems. In: Proceedings of the Ninteenth IFAC World Congress, vol. 10, pp. 1977–1984. Cape Town, South Africa (2014). doi:10.3182/20140824-6-ZA-1003.01992
13. Kothari, M., Manathara, J.G., Postlethwaite, I.: Cooperative multiple pursuers against a single evader. J. Intell. Robot. Syst. **86**, 1–17 (2016). doi:10.1007/s10846-016-0423-3
14. Ramana, M.V., Kothari, M.: Pursuit strategy to capture high-speed evaders using multiple pursuers. J. Guid. Control Dyn. **40**, 139–149 (2016). doi:10.2514/1.G000584
15. Ramana, M.V., Kothari, M.: Pursuit-evasion games of high speed evader. J. Intell. Robot. Syst. **85**, 1–14 (2016). doi:10.1007/s10846-016-0379-3
16. Cockayne, E.: Plane pursuit with curvature constraints. SIAM J. Appl. Math. **15**(6), 1511–1516 (1967). doi:10.1137/0115133
17. Pachter, M., Getz, W.M.: The geometry of the barrier in the game of two cars. Optim. Control Appl. Methods **1**(2), 103–118 (1980). doi:10.1002/oca.4660010202
18. Rublein, G.: On pursuit with curvature constraints. SIAM J. Appl. Math. **10**(1), 37–39 (1972). doi:10.1137/0115133
19. Merz, A.: The game of two identical cars. J. Optim. Theory Appl. **9**(5), 324–343 (1972). doi:10.1007/bf00932932
20. Getz, W.M., Pachter, M.: Capturability in a two-target game of two cars. J. Guid. Control Dyn. **4**(1), 15–21 (1981)
21. Pachter, M., Miloh, T.: The geometric approach to the construction of the barrier surface in differential games. Comput. Math. Appl. **13**(1), 47–67 (1987)
22. Exarchos, I., Tsiotras, P., Pachter, M.: UAV collision avoidance based on the solution of the suicidal pedestrian differential game. In: AIAA Guidance, Navigation, and Control Conference, San Diego, CA. American Institute of Aeronautics and Astronautics (AIAA) (2016). doi:10.2514/6.2016-2100
23. Exarchos, I., Tsiotras, P., Pachter, M.: On the suicidal pedestrian differential game. Dyn. Games Appl. **5**(3), 297–317 (2015). doi:10.1007/s13235-014-0130-2